THESIS OF DOCTORAL (PhD) DISSERTATION

AMBRUS BÁLINT

MOSONMAGYARÓVÁR

2023

THESIS OF DOCTORAL (PhD) DISSERTATION

SZÉCHENYI ISTVÁN UNIVERSITY
ALBERT KÁZMÉR FACULTY OF MOSONMAGYARÓVÁR
Department of Biosystems and Precision Technology

Antal Wittmann Multidisciplinary Doctoral School of Plant, Animal and Food Sciences

Head of the Doctoral School: Prof. Dr. László Varga DSc
professor

Program: Gottlieb Haberlandt Plant Sciences Doctoral Program
Program leader: Prof. Dr. Gyula Pinke DSc
professor

Supervisors:
Dr. Anikó Nyéki PhD
associate professor,

Dr. Gergely Teschner PhD
assistant professor

DEVELOPMENT OF DATA COLLECTION TECHNOLOGIES IN PRECISION CROP PRODUCTION, REGARDING TO AUTONOMOUS EQUIPMENT

Written by:
AMBRUS BÁLINT

MOSONMAGYARÓVÁR
2023

1. INTRODUCTION

The dissertation presents an autonomous smart intelligent data collection and analysis robot, which is capable of sensing the environmental parameters and processing RGB images using machine learning method. The robot's sensing, data processing and data transmission system has been enhanced thoroughly. The development goal was to create a low-cost and multifunctional mobile field robot for precision agriculture.

The other aim of the research was to estimate the number the yield of tomatoes with the self-developed robot and a digital single-lens reflex (DSLR) camera. In open-field and in greenhouse condition, in addition to indoor and outdoor cultivation technology. The thesis proposes a new approach for tomato yield prediction, based on RGB images, 3D scanning and modelling. A convolutional neural network (CNN) model was developed for tomato segmentation.

2. MATERIAL AND METHOD

2.1. Basic robot system

The original robot system is the XiaoR Geek TH Robot Car Kit type open source robot platform. The robot walking structure has a rubber belt design. The central unit is a Raspberry Pi 4 microcomputer. The robot is equipped with a robotic arm with four degrees of freedom, which can be moved in two mutually perpendicular directions with servomotors. It is also equipped with an RGB camera that can be positioned along two axes with servomotors. The robot's control software was created in the Python programming language. The device can be operate via a wired or wireless connection.

2.2. Robot development

The frame structure elements were expanded for field work, and the motors of original driving motors were replaced with higher performance motors.

The power supply is provided by a Li-Ion battery pack. Lower voltage systems are supplied by converters.

An artificial intelligence module was installed on the central unit of the robot, which can classify the images of the RGB camera. This method uses a neural network model created with the Edges Impulse platform using the TensorFlow software library.

The robot is controlled by a self-developed application, which can reached all functions of the robot.

The robot is equipped with sensors: global radiation, ambient temperature, humidity, soil surface infrared thermometer, soil temperature, soil moisture content, EC, pH and NPK content.

The equipment has a LiDAR which is responsible for autonomous movement and the GPS receiver stored the position of the robot.

2.3. Experimental locations

The open-field experiment was located at the Hungarian University of Agricultural and Life Sciences in Gödöllő. Five treatments were set up in two replicates and each was associated with two sampling sites.

The other experiment was under greenhouse conditions at Dunakiliti owned by Ranyak Family Horticulture Ltd. The plants were grown using a vertical technology. We collected data from 27 sample locations.

2.4. Data collection and processing methods

The pictures were taken with a 12.2 Megapixel Canon EOS 1100D (DSLR) camera with a sensor size of 22.2×14.8 *mm*, in the RGB color range.

In the field experiment, the photographs were taken in full manual camera mode at a distance of 100 cm above the tomato plants using a camera stand. For the data analysis, we used a dataset consisting of 5 RGB images align together into a panoramic image at each sampling location, thus giving an image of the entire sampling location. In the greenhouse experiment, the pictures were taken in side view at a distance of 100 *cm* from the rows of plants using a camera stand, with the camera settings used in the open-field experiment.

Image data collection was also done with the help of a 1.3 Megapixel 3.00×4.32 *mm* sensor size camera integrated into the robot. In the case of the open-field and greenhouse experiments, the robot took the recordings from one direction at a distance of 40 *cm* from the plant rows. In the open-field experiment, the recording was done in one step, the completed images were

also combined into panoramic images. In the case of the greenhouse experiment, due to the height of the plants, the recording was done in two steps, with a camera position of 0° and 45°.

2.4.1. Image processing methods

Two methods were used to process the images. Firstly, we created a representative dataset and two classes using a total of 924 images; ripe and row tomato groups. The Edge Impulse system did not work directly online with the robot, but instead ran a standalone application. Due to the computing capacity, the frame rate was a maximum of 5 FPS, which proved to be sufficiently given the low speed of the robot.

As another method of image processing, we used a post-processing method using an OpenCV procedure. This procedure uses color separation, LiDAR distance data and preliminary parameters of the tomato crop.

Figure 1 illustrates the steps of the machine vision-based image processing method based on DSLR camera recordings. Steps of the image data evaluation method identical for both platforms.

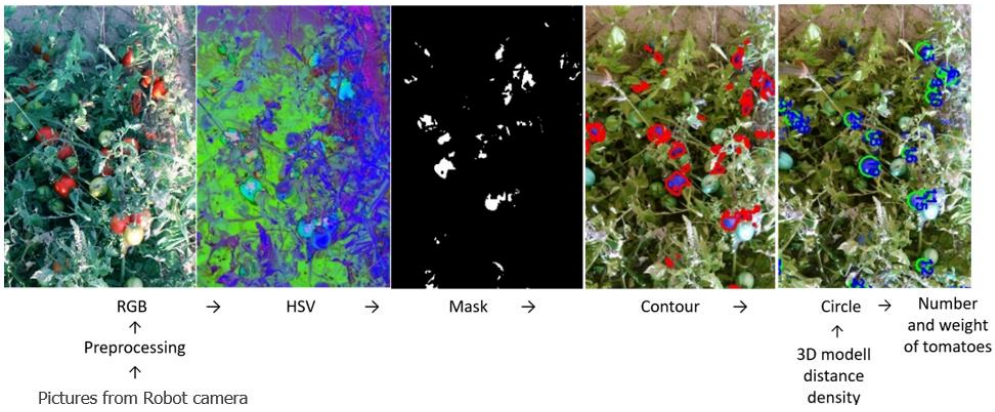

1. Figure - Steps of the image data evaluation method

2.5. Correction methods for image processing

Lens correction: The DSLR camera lens disortion was known, therefore, no calibration was performed in this case. In the case of the robot, during the calibration, we used a checkerboard pattern calibration panel, which consists of 91 white and black squares with a side length of 10 *mm*. The robot's camera took photos of the calibration panel from different arbitrarily chosen distances and angles.

During the ***distance calibration*** measurement, we took pictures of a reference object, which was a red circle with a known surface, using both data collection platforms. Our goal was to determine the relationship between the real surface (cm^2) of the reference object and the surface (*pix*) defined in the recordings. The images were taken with the same camera settings at distances between 20 and 200 *cm* in 10 *cm* increments.

During the color and light correction test, we took 15 pictures with the same settings of the 4 ripe tomato samples collected from the greenhouse experiment. To determine the color segmentation values, we used images of the tomato crop taken at 15 different illumination values using histograms representing the separate channels of the images. The characteristic colors of the image were extracted from the histograms and the HSV values of these colors were used to determine the segmentation intervals.

2.6. Method of 3D modelling of tomato crop

To create the 3D model of the tomato crop, we used a retrofitted free source Ciclop 3D laser scanner. After the device was calibrated, the actual scanning took place. The desired object was placed in the center of the scanning platform so that it pointed towards both lasers.

In both measurement areas, the fruit samples were randomly selected, making sure that all samples were in the same state of ripeness. After the scanning process, a 3D point cloud was created that represents the morphological characteristics of both tomato varieties. Based on the point cloud, we produced a closed-surface 3D model of the crops using Horus software.

3. RESULTS

3.1. Results of robot development

The robot (Figure 2) is able to autonomously guide between the rows. It uses the RPLIDAR A1 type laser sensing module what can make measurements in defined direction and calculate distance data. If the measured distance is less than a preset value, then the robot can move opposite direction. During the field application, the deviation was ±2 *cm* in average.

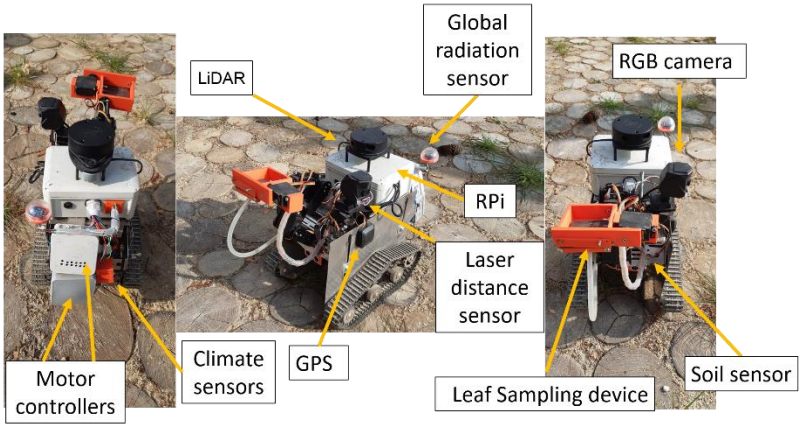

2. Fig. – With the main components of the robot

The equipment can record the collected data in tabular form in its own memory, but it also capable to store on GSM-based cloud storage. ThingSpeak (an online IoT analysis platform service) was used to store the data.

3.2. Results of 3D modelling of tomato crops

In order to estimate the yield of tomatoes, we developed a model of the tomato crop with a 3D scanner. After determining the volumes of the tomato model, we added the best-fitting spheres using the least-squares method to approximate the berries for yield estimation. We performed the yield estimation by processing the images considering the ratio of the volume of the

sphere to the volume of the tomato berries as a correction factor, as well as the average density of the tomato fruit.

3.3. Optical correction results

Adobe Lens Profile Creator 1.0.4 software was used during the lens correction method, which created a calibration matrix based on the images taken by the robot from different directions and distances of the calibration sample. The program corrects the images for perspective view using the distortion coefficients.

An OpenCV-based technique was used to process the images during the light correction and color tests. The values of the segmentation interval can be determined with the HSV minimum and maximum values, which represent the HSV parameters of the ripe tomato. It can be concluded, that the size of the designated area begins to decrease at values lower than 3000 *lx* illumination.

Color segmentation was used after eliminating the lens desorting in the distance calibration. We separated and marked the objects and we determined the measured surface area in pixels. After that, this number was divided by the surface area of the reference object in cm^2. The result is a ratio in $pix\ /\ cm^2$ that can be used to determine the real surface area of the ripe tomatoes using the LiDAR distance data.

3.3. Image processing results

3.3.1. Results of the tomato crop detection method

During the movement of the robot can be analyzed the recorded images by a machine learning-based CNN (Figure 3). The F1 performance indicator value of the model was more than 90%, indicating that the model correctly predicts all tomatoes berries.

3. Figure - Detected tomato berries

3.3.2. Results of the yield estimation method

The results of the DSLR camera images are the open-field experiment. We determined the total weight of the tomato berries by approximating the sphere ($\overline{m_1}$) and the 3D model ($\overline{m_2}$), with R^2 values of 0.73 and 0.98 (Figure 4).

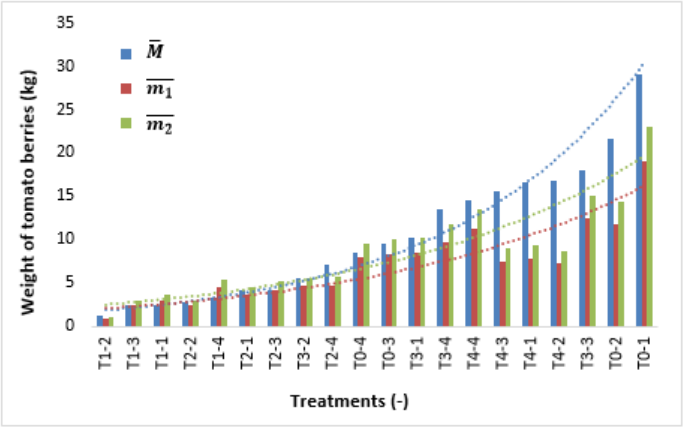

4. Figure - Comparison of tomato berry weight based on the increasing yield each treatment.

The average of the calculated weight showed smaller values than the measured tomato weight. The average relative error of the method was 21.90% smaller than in the case of the 3D model, the error of approximation with a sphere, which was 25.52%.

The results of the DSLR camera images are the greenhouse tomato experiment. We obtained the total weight of the tomato berries for each sample plant, using the sphere for the first measurement ($\overline{m_3}$), second measurement ($\overline{m_5}$) and the 3D model for the first measurement ($\overline{m_4}$), second measurement ($\overline{m_6}$) by approximation (Figure 5).

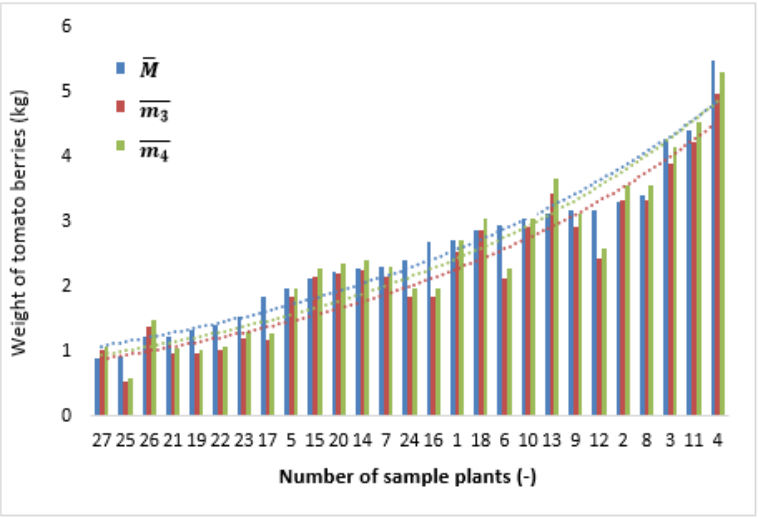

5. Figure - Comparison of tomato berry weight based on the increasing yield of treatment at the first measurements date

The average relative error of the method was smaller applying the 3D model, than the error of approximation with the sphere model. However, some overestimation were observed, this error is due to surface designation and the overlapping of the tomato berries and leaves. The best relative error of the measurements was 9.95%.

The results of the robot's images are the open-field tomato experiment: The robot took a total of 453 images during harvesting. We obtained the weight data of the approximation with the sphere ($\overline{m_7}$) and the 3D model ($\overline{m_8}$) as the

final product. In the case of approximation with both models, the correlation for each treatment is between 0.77 and 0.95 R^2 values (Figure 6).

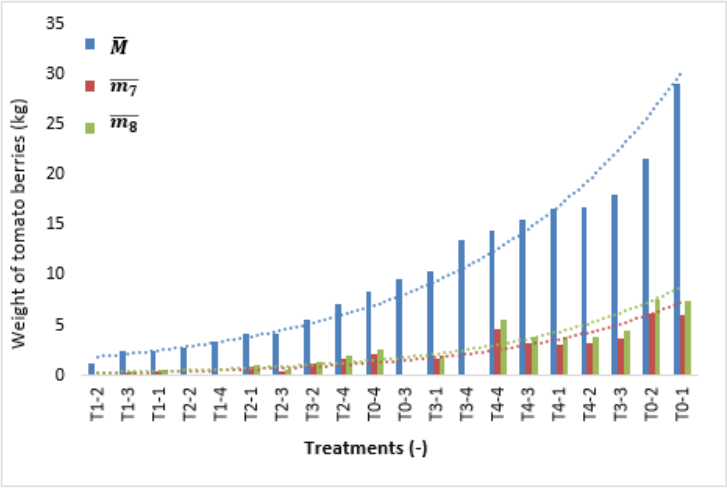

6. Figure - Comparison of tomato mass based on different methods based on the increasing yield of treatments

The high relative error values of 76.07% and 80.22% were caused by the image recording method, because the vegetation of the tomatoe rows was recorded only from one side. We didn't have information about the other side of the rows.

The results of the robot's images are the greenhouse tomato experiment. We obtained the tomato weight by approximating with the sphere model the first measurement ($\overline{m_9}$) and second measurement ($\overline{m_{11}}$), and with the 3D model the first measurement ($\overline{m_{10}}$) and second measurement ($\overline{m_{12}}$). The correlation coefficient was 0.9029 in the first measurements time, and 0.8473 R^2 in second measurements time in all treatments with two different models. It is equivalent with the correlation results with DSLR camera (Figure 7).

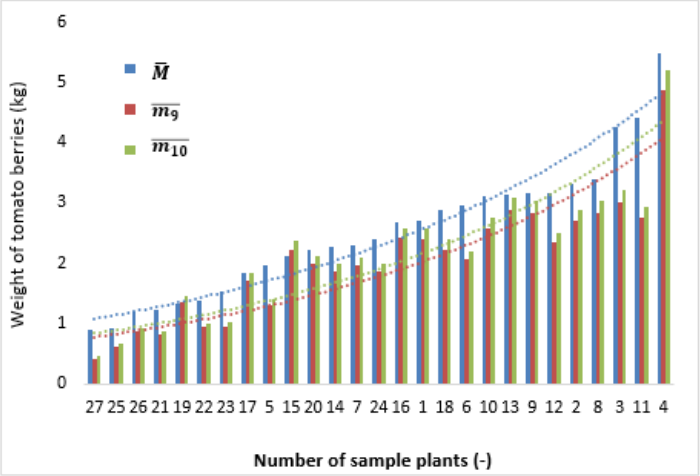

7. Figure - Comparison of tomato berry weight based on the increasing yield of each treatment at the first measurement

We obtained more significant results using the 3D model at both measurements time. The best relative error of the measurements was 17.07%.

Table 1 illustrates the summary results of the yield determination for open-filed and for greenhouse.

1. Table - The experiments yield data

	Platform (-)	**Approximation (-)**	$\bar{M}$ **(kg)**	$\overline{m_x}$ **(kg)**	$\bar{x}$ **(kg)**	***Hx* (kg)**	***hx* (%)**
Open-field measurement	DSLR	Sphere	10.35	$\overline{m_1}$	7,10	3.42	25.52
		3D		$\overline{m_2}$	8.59	2.45	21.90
	Robot	Sphere		$\overline{m_7}$	2.42	8.69	80.22
		3D		$\overline{m_8}$	2.93	8.18	76.07
1st greenhouse measurement	DSLR	Sphere	2.52	$\overline{m_3}$	2.27	0.30	14.03
		3D		$\overline{m_4}$	2.43	0.25	12.62
	Robot	Sphere		$\overline{m_9}$	2.02	0.51	21.48
		3D		$\overline{m_{10}}$	2.16	0.39	17.07
2nd greenhouse measurement	DSLR	Sphere	1.23	$\overline{m_5}$	1.07	0.17	13.72
		3D		$\overline{m_6}$	1.15	0.13	9.95
	Robot	Sphere		$\overline{m_{11}}$	0.88	0.35	27.92
		3D		$\overline{m_{12}}$	0.95	0.29	22.88

3.3.3. Results of determination of tomato berry number

The results of DSLR camera images are the open-filed experiment.

We get the calculated tomato yield ($\overline{n_1}$) for the determine treatments. The degree of linear relationship were between 0.8831 and 0.9965 R^2 for the treatments (Figure 8).

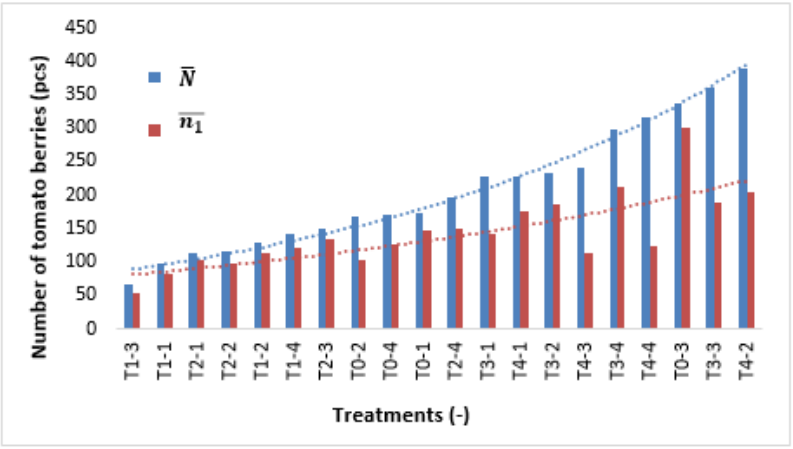

8. Figure - Comparison of tomato numbers based on the increasing yield of treatment.

The average deviation was 71 pieces of tomato berries from the actual number of pieces, while the average relative error was 28.57%, so the method greatly underestimated the real value.

The results of DSLR camera images are the greenhouse tomato experiment. We determined the calculated tomato yield at the first measurement ($\overline{n_2}$) and the second measurement ($\overline{n_3}$). The R^2 values were 0.9545 and 0.8667 which is similar to the coefficients of the determine weight at the measurements date (Figure 9).

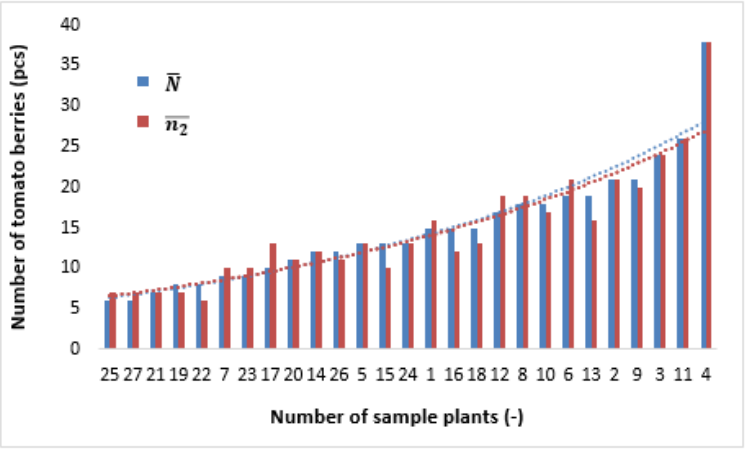

9. Figure - Comparison of tomato number and increasing yield of sample plants based at the first measurement

The deviations of the actual value deviations are similar in the case of weight yield determination and also in the berries number calculation. The average of the absolute error was 1 tomato berrie which means 9.20% average relative error at the first measurement. The more accurate detection results were caused by the vertical cultivation technology.

The results of the robot's images are the open-field experiment. We established the calculated tomato yield using the segmentation procedure ($\overline{n_4}$) and based on CNN ($\overline{n_5}$) too for all treatments (Figure 10).

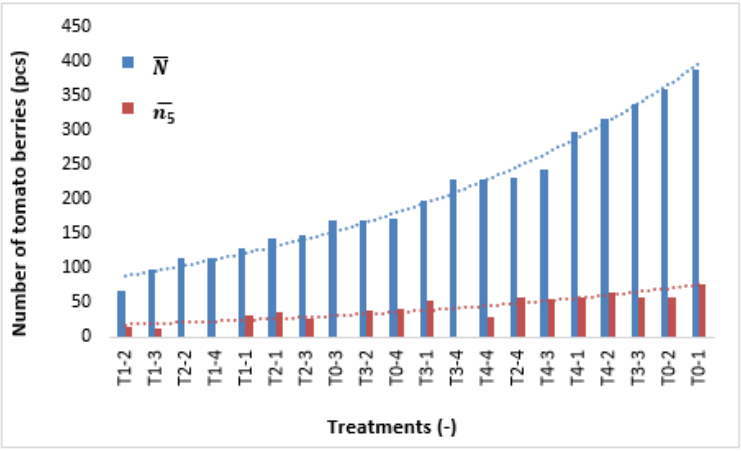

10. Figure - Comparison of tomato yield based on segmentation from robot camera images

The determination coefficients were between 0.4945 and 0.9422 using CNN for all treatments. These values were between 0.618 and 0.870 R^2 with the segmentation method for each treatments. The coefficient was 0.7849 R^2 value in the case of the segmentation procedure while 0.8069 R^2 value was extracted using the CNN analysis examining the whole measurements. More than 80% underestimation were characterized in both methods. The reason of the result's discrepancy can be found at the detection methods.

We found almost the same average error with values of 175 and 172 during the examination procedures. The relative error average was also high, 84 and 83. Thus, the results of the two methods are approximately the same. The CNN model show slightly better results.

The results of the robot's images are the greenhouse experiment.

We determined the calculated tomato yield using two different methods as well. We calculated the ($\overline{n_6}$) value for the first measurement and ($\overline{n_8}$) for the second measurement based on CNN method for all sample locations. Then we determined ($\overline{n_7}$) the first measurement and ($\overline{n_9}$) for the second measurement

values based on segmentation projected onto sampling locations. The segmentation method gave more progressive results in both measurements. The R^2 value was 0.9145 for the first measurement time, while 0.8394 for the second date covering the all sample plants (Figure 11).

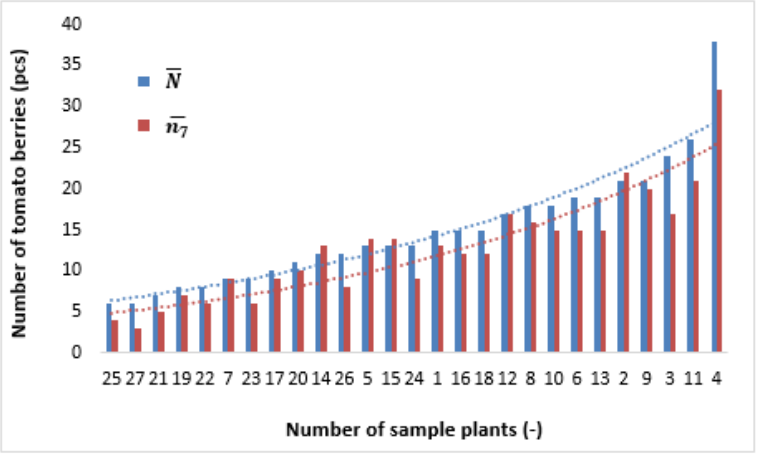

11. Figure - Comparison of tomato number based on the increasing yield of sample plant with the segmentation method at the first measurement date

We obtained similar results of the DSLR camera pictures for both methods. In contrast to the field experiment, the results did not show such a high level of underestimation. The average relative error ranged were between 18.02% and 32.35%.

Table 2 illustrates the results of the crop number determination in the open-field and in the greenhouse.

2. Table – Cumulative tomato yield in both experiments

	Analysis method (-)	Platform (-)	$\bar{N}$ (pcs)	$\overline{n_y}$ (pcs)	$\bar{x}$ (pcs)	H_i (pcs)	hy (%)
Open-field measurement	Segmentation	DSLR	207.5	$\overline{n_1}$	136.6	70.9	28.5
	Segmentation	Robot		$\overline{n_4}$	41	175	84.2
	CNN	Robot		$\overline{n_5}$	44.8	171.7	83.3
1st greenhouse measurement	Segmentation	DSLR	14.9	$\overline{n_2}$	14.7	1.1	9.2
	CNN	Robot		$\overline{n_6}$	11.4	3.5	23.1
	Segmentation	Robot		$\overline{n_7}$	12.7	2.4	18.0
2nd greenhouse measurement	Segmentation	DSLR	20.8	$\overline{n_3}$	18.7	2.7	12.6
	CNN	Robot		$\overline{n_8}$	14.1	6.7	32.3
	Segmentation	Robot		$\overline{n_9}$	14.7	6.0	28.2

4. NEW SCIENTIFIC RESULTS (THESES)

1. **I proved that the determined color segmentation interval – can give accurate selection for the ripe tomato berries, under higher illumination value of 3000 lx – after applying calibration methods for images errors.**
2. **I proved that tomato yield predictions can be calculated for open-field and for greenhouse conditions with the developed pixel/metric and LiDAR-based measurement of the distance of the object, by determining the size of the surface of the object projected onto a parallel plane placed at the distance of the object, and by creating a model of tomato berries varieties scanned in 360° based on preliminary 3D scanning.**
3. **I proved that a more accurate (with an average 3.73%) tomato yield estimation can be allow with the 3D scanning technology than the morphological approximation with a sphere correction model under the investigated conditions.**
4. **I proved that the convolutional neural network (designed with 8-bit quantization) can be operable from on-the-go clustering and counting tomato plant parts with a 5 FPS data processing capacity by relative error of 23.18% based on robot's images. Besides the tomato berries number determination could work with 7.25% average relative error with machine vision technic contrary to the neural network.**
5. **I verified that an average of 28.08% better results could be reach with the extraction by the 12.2 Megapixel 22.2×14.8 *mm* sensor size DSLR camera than uding the robot's 1.3 Megapixel of 3.00×4.32 *mm* sensor size camera images, with the same settings and machine vision**

processing treatment. So I proved, that tomato berries and yield estimations are significantly affected by image recording processes.

PRACTICAL APPLICABILITY OF THE THESIS

1. I developed a commercially available open source robot with hardware and software, and added sensors as well as actuators for in precision agriculture.
2. The developed robot results show that the system can be used with both open-field and greenhouse technology. It is capable expanded for both data collection and intervention, regarding the possibilities provided by the modular structure. It can be integrated into modern precision technologies because of the cloud-based storage of the data.
3. The robot provides support for the big data-based growth and forecasting models with artificial intelligence.
4. The 3D scanning process is suitable for accurate yield estimation, even for other crops.
5. I carried out developments covered the remote sensing, data collection, sensing and robotics topics in precision crop production during my research, that proven to be applicable in horticulture and may be the basis of R&D projects.

5. LIST OF PUBLICATIONS

I. SCIENTIFIC PUBLICATIONS PUBLISHED IN FOREIGN LANGUAGES

Ambrus, B. – Teschner, G. – Kovács, A.J. – Neményi, M. – Helyes, L. – Pék, Z. – Takács, S, **–** Alahmad, T., Nyéki, A. 2023. Field-grown tomato yield estimation using point cloud segmentation with 3D shaping and RGB pictures from a field robot anddigital single lens reflex cameras. Heliyon (*Under Print*). IF: 3.776, Q1.

Kulmány, I. M. **–** Bede-Fazekas, Á. **–** Beslin, A. **–** Giczi, Zs. **–** Milics, G. – Kovács, B. **–** Kovács, M. **– Ambrus, B**. – Bede, L. **–** Vona, V. 2022. Calibration of an arduino-based low-cost capacitive soil moisture sensor for smart agriculture. Journal of Hydrology and Hydromechanics 70(3). IF: 2.329, Q1.

Neményi, M. – Kovács, A.J. – Oláh, J. –Popp, J. – Erdei, E. – Harsányi, E. – **Ambrus, B. –** Teschner, G. – Nyéki, A. 2022. Challenges of sustainable agricultural development with special regard to internet of things: survey. Progress in Agricultural Engineering Sciences 18(1). IF: 0.43, Q4.

Nyéki, A. – Teschner, G. – **Ambrus, B. –** Neményi, M. – Kovács, A.J. 2020. Architecting farmer - centric internet of things for precision crop production. Hungarian agricultural engineering. 38.

II. SCIENTIFIC PUBLICATIONS PUBLISHED IN HUNGARIAN LANGUAGE

Ambrus, B. 2021. A robottechnika alkalmazási lehetőségei a szántóföldi növényvédelemben. Acta agronomica óváriensis 62(1).

Molnár, J. **– Ambrus, B. –** Zsédely, E. 2014. Minőségi élelmiszerek fogyasztásának szerepe az egészség megőrzésében. Élelmiszer tudomány technológia 68.

III. MATERIALS OF SCIENTIFIC CONFERENCES PUBLISHED IN FULL

Ambrus, B. – Teschner, G. – Neményi, M. – Nyéki, A. 2022. Self-developed small robot for tomato plants detection In: 2nd African Conference on Precision Agriculture.

Ambrus, B. – Teschner, G. – Kovács, A. J. – Neményi, M. 2022. Development of small smart data logger robots embedded in IoT system for crop production. In: International Scientific Conference „Agricultural mechanization and technology in Europe and perspectives“ proceeding : Tiblisi.

Teschner, G. – **Ambrus, B. –** Nyéki, A. – Neményi, M. – Kovács, A. J. 2018. Lézeres detektáláson alapuló kukorica tőközművelő eszközfejlesztés In: XXXVII. Óvári Tudományos Napok, 2018. november 9-10.: Fenntartható agrárium és környezet, az Óvári Akadémia 200 éve - múlt, jelen, jövő.

Tolner, I. T. – **Ambrus, B**. – Szalay, K.D. 2017. Software base system model, ANSYS Fluent of developed bubble column (Air lift) Tubular photobioreactor. In: Nyéki, Anikó; Kovács, Attila József; Milics, Gábor (szerk.) Towards sustainable agricultural and biosystems engineering.

Neményi, M . – Milics, G. – Tolner, I. – **Ambrus, B. –** Rétfalvi, T. – Kovács, A.J. 2015. Contribution to the technological development of microalgae production in Hungary. In: Ördög, V; Molnár, Z (szerk.) 7th Symposium on Microalgae and Seaweed Products in Plant/Soil-Systems "Contribution to Sustainable Agriculture.

IV. ABSTRACTS PUBLISHED IN SCIENTIFIC CONFERENCE PUBLICATIONS

Ambrus, B. – Nyéki, A. 2023. Small autonomous robot development for data logging and analyzing.

Ambrus, B. – Nyéki, A. – Teschner, G. – Neményi, M. – Milics, G. – Kovács, A.J. 2021. Agro iot platforms and sensors in crop production. In: Stafford, J. V.; Milics, G (szerk.) Book of abstracts of all the posters.

Neményi, M. – Nyeki, A. – Nagy, J. – Harsányi, E. – Teschner, G. – **Ambrus, B**. – Milics, G. – Kovács, A.J. 2018. Internet of Thing (IoT) for ecological sustainability in precision crop production.

V. ANNOUNCEMENTS PUBLISHED IN HUNGARIAN LANGUAGE

Ambrus, B. – Neményi, M. – Kovács, A.J. – Nyéki, A. 2022. Small-smart robot fejlesztése mosonmagyaróváron, Mezőgazdasági technika.